Chemistry–A European Journal
Communication
doi.org/10.1002/chem.202005191

Chemistry Europe
European Chemical Societies Publishing

C–H Functionalization |*Hot Paper*|

Novel Arylindigoids by Late-Stage Derivatization of Biocatalytically Synthesized Dibromoindigo

Christian Schnepel,[a, b] Veronica I. Dodero,[a] and Norbert Sewald*[a]

Abstract: Indigoids represent natural product-based compounds applicable as organic semiconductors and photoresponsive materials. Yet modified indigo derivatives are difficult to access by chemical synthesis. A biocatalytic approach applying several consecutive selective C–H functionalizations was developed that selectively provides access to various indigoids: Enzymatic halogenation of L-tryptophan followed by indole generation with tryptophanase yields 5-, 6- and 7-bromoindoles. Subsequent hydroxylation using a flavin monooxygenase furnishes dibromoindigo that is derivatized by acylation. This four-step one-pot cascade gives dibromoindigo in good isolated yields. Moreover, the halogen substituent allows for late-stage diversification by cross-coupling directly performed in the crude mixture, thus enabling synthesis of a small set of 6,6′-diarylindigo derivatives. This chemoenzymatic approach provides a modular platform towards novel indigoids with attractive spectral properties.

Indole is a widespread heterocycle found in many natural products.[1] For instance, indigo dyes derived from indole have been applied in textile dyeing for thousands of years due to their outstanding spectral properties.[2,3] Indigo (**1**) developed to a bulk chemical in the last century whereas its C6-brominated analogue, 6,6′-dibromoindigo (6,6′-**2**), the major component of the high-value pigment Tyrian purple, still remains a rarity (Scheme 1 A). Thanks to tremendous efforts by several research groups traditional indigoids recently turned into focus as natural product-based, non-toxic materials for sustainable organic electronics.[4–6] Topical studies examining the photoswitching abilities of *N*,*N*′-aryl-substituted indigos pointed to a useful strategy to tailor their photochemical properties.[7–9] Synthetic routes towards **1** were developed by Baeyer and by Heumann and paved the way to multi-ton production, yet its dibrominated counterpart **2** has never entered an industrial scale production.[10]

Today biocatalysis offers a versatile methodology to address selectivity issues, e.g., arising from similarly reactive C–H moieties.[11] Recent advancements on enzyme discovery, engineering as well as tremendous efforts on process development open up elaborate transformations that can be carried out under mild conditions, often with excellent selectivities.[12–14] Immense progress has been achieved in enzyme-catalyzed C–H functionalization.[15] Especially oxyfunctionalization is a paramount approach to activate C–H bonds by using biocatalysts that are capable of utilizing molecular oxygen. Manifold biocatalytic approaches in this rapidly evolving field, especially on the use of P450 enzymes, were extensively reviewed, giving a wide overview on the current state of the art.[16–19] The first fermentative synthesis of indigo was reported by Ensley and later by Lee et al. using a dioxygenase for indole hydroxylation. Tryptophanase that originated from endogenous tryptophan catabolism was exploited to obtain indole.[20,21] Heme-dependent monooxygenases (MOs) were later evolved towards C3-hydroxylation of indole.[22–24] Flitsch et al. used formation of indigo-derived pigments for detecting activity of MO mutants.[25,26] Biocatalytic functionalization of unprotected indole was achieved using engineered myoglobin variants which catalyze non-native carbene transfer in whole cells.[27] Besides using heme-dependent enzymes, also flavin-dependent MOs play a key role in oxyfunctionalization. Accordingly a flavin monooxygenase from *Methylophaga* sp. (mFMO) was established for the biotechnological production of indigo and indirubin.[28,29] Nevertheless, the synthesis of valuable halogenated indigos has remained on analytical or small preparative scale, particularly due to the low efficiency of halogenases as a severe bottleneck. In more recent studies, Tischler and co-authors reported on the conversion of haloindoles using a small array of styrene MOs.[30] One-pot synthesis of indigoids either in bacteria or plant as the hosts was recently achieved: By introducing a tryptophan halogenase into the host strain along with a hydroxylase, production of indigoids from tryptophan was feasible, omitting the need for costly substituted indole substrates through exploiting the cellular metabolism.[31,32] However, product titers remained low and the isolation of the pigment from the cultivation broth can become a tedious procedure. Moreover, structural modifications that can be, for ex-

[a] *Dr. C. Schnepel, Dr. V. I. Dodero, Prof. Dr. N. Sewald*
Organische und Bioorganische Chemie, Fakultät für Chemie
Universität Bielefeld, Universitätsstraße 25, 33615 Bielefeld (Germany)
E-mail: norbert.sewald@uni-bielefeld.de

[b] *Dr. C. Schnepel*
Present address: School of Chemistry
Manchester Institute of Biotechnology, The University of Manchester
131 Princess Street, Manchester, M1 7DN (UK)

Supporting information and the ORCID identification number(s) for the author(s) of this article can be found under: https://doi.org/10.1002/chem.202005191.

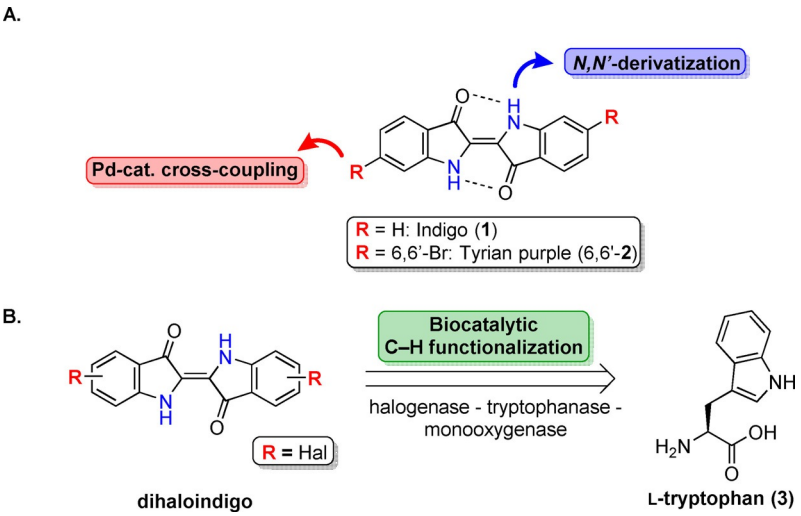

Scheme 1. A. Structure of natural indigo dyes and diversification strategies. B. Biocatalytic retrosynthesis of haloindigo via multiple steps of C–H functionalization.

ample, introduced by chemocatalysis, prove challenging when applying whole cell catalysts. As an alternative, in vitro enzyme cascades offer a more modular approach for scaffold diversification.

We embarked on the development of a modular biocatalytic platform to afford the synthesis of haloindigo that can be easily isolated and/or diversified by addressing the halogen substituents using Pd-catalyzed cross-coupling. Assembly of the indigoid scaffold is achieved by stepwise C–H functionalization utilizing selective halogenation and hydroxylation starting from L-tryptophan (**3**, Scheme 1 B).[15] Various recent achievements underscore that flavin-dependent tryptophan halogenases are capable of regioselective aryl halogenation using O_2, $FADH_2$ and a halide salt.[33,34] Current efforts on random and targeted engineering, immobilization and combination with chemocatalysis considerably extended the synthetic utility of these enzymes.[35–40] Recent reports also showcase applications of halogenases for the synthesis of valuable chemicals using cascades in vivo and in vitro.[41–43] However, reports on enzymatic halogenation of free indole indicate that the substitution usually occurs in the electronically most favored C3 position.[44] To retain regioselectivity at the benzene ring, it is necessary to halogenate L-tryptophan (**3**) instead, since the toolkit of regiocomplementary halogenases allows to specifically address the C5-, C6-, or C7-position of the indole moiety (Scheme 2).

Formation of crosslinked enzyme aggregates (CLEAs) enables preparative-scale bromination of **3** resulting in product titers of 280 mg L^{-1}. As demonstrated in earlier studies, CLEAs permit facile upscaling of the halogenation reaction. The brominated amino acid is selectively obtained whereas protein contaminants are simply filtered, therefore providing a good starting point for cascade reactions.[38] In the next step, tryptophanase catalyzes the cleavage of the amino acid backbone to release bromoindole (**5**): In a pyridoxal phosphate-dependent reaction, a 1,4-elimination takes place leading to **5** and pyruvate. The gene encoding the tryptophanase TnaA (EC 4.1.99.1) from *E. coli* was subcloned, and the resulting enzyme was utilized in biotransformations (Figure S1, S2).[45,46] Initially, the activity of TnaA towards L-6-bromotryptophan (6-**4**) was confirmed in analytical-scale reactions. Upon incubation of 6-**4** with purified TnaA, 6-bromoindole (6-**5**) was successfully formed (Scheme S3). This motivated performing TnaA-catalyzed elimination preceded by enzymatic halogenation in a one-pot fashion on a milligram scale (Figure 1). After quantitative halogenation of 3 (0.1 mmol) using the C6-halogenase Thal along with auxiliary enzymes (combiCLEAs) a cell-free extract containing overexpressed TnaA was simply added to the

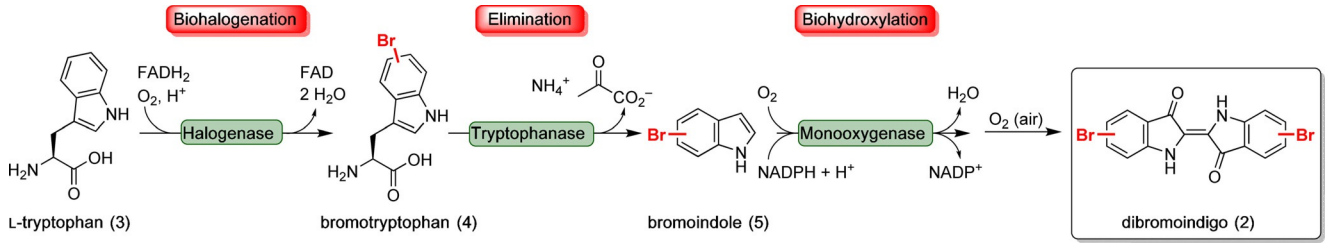

Scheme 2. General overview of the enzyme cascade for the synthesis of brominated indigo dyes starting from L-tryptophan (**3**). Sequential C–H activation was initiated by enzymatic halogenation of the indole side chain occurring selectively at C5, C6, or C7, respectively. Elimination of the amino acid backbone and final hydroxylation at C3 position that spontaneously dimerizes gives target compound **2**.

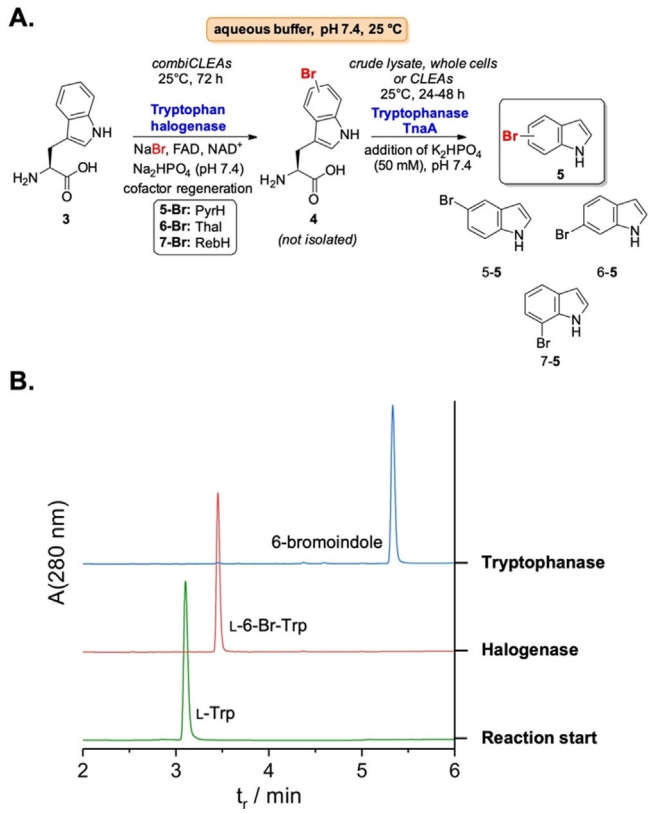

Figure 1. A. One-pot synthesis of 5-, 6-, and 7-bromoindole, respectively, by sequential combination of halogenase and tryptophanase. B. Cutout of RP-HPLC traces of two-step biocatalysis highlighting the selective synthesis of 6-bromoindole (6-**5**) starting from Trp by sequential halogenation and elimination.

biotransformation mixture. Moreover K_2HPO_4 was added to a final concentration of 50 mM because potassium cations were reported to have a positive impact on TnaA,[47] whilst K^+ ions were omitted during halogenation to suppress undesired activity of endogenous tryptophanase. By incubation for 24 h at 25 °C, >98% of substrate was selectively converted into 6-bromoindole (6-**5**), thus avoiding intermediary isolation of 6-**4** (Figure 1 B). Notable side products did not occur, which indicates the high selectivity of the consecutive biotransformations to isolate haloindoles in two steps that can be hardly synthesized otherwise.

By applying TnaA crude lysate, freeze-dried cells or CLEAs, haloindoles were afforded in quantities sufficient for multistep synthesis and characterization (Table 1; Figure S4). 5-, 6-, and 7-bromo isomers of **5** hence are obtained with >90% conversion on larger scale. Solely, the TnaA loading had to be increased in case of 7-**5**, presumably due to a lower activity. Final isolation of **5** merely requires desalting over a plug of reversed-phase silica leading to a satisfying product purity of >95% (Figure S5). Application of this cascade provides 5-, 6- and 7-bromoindole (**5**) in good yields ranging from 60–70% for two synthetic steps, starting from **3**.

Inspired by these results, 6-**5** was subjected to enzyme-catalyzed C3-hydroxylation. The flavin-dependent monooxygenase (mFMO) from *Methylophaga* spp. was cloned and established

Table 1. Results of enzymatic synthesis of bromoindole applying a sequential cascade of halogenation and TnaA-catalyzed elimination. Different halogenated regioisomers were obtained by choosing regiocomplementary halogenases (5-Br: PyrH; 6-Br: Thal; 7-Br: RebH) in the first step (Figure 1 A).

#	Product isomer (5)	TnaA formulation	Scale [mmol]	Conversion,[a] total yield[b]
1	6-Br	crude lysate (0.15 L *E. coli* culture)	0.10	98%, *not isolated*
2	6-Br	CLEA (1.5 L *E. coli* culture)	1.0	>99%, 60%
3	6-Br	freeze-dried cells (1 mg mL^{-1})	0.25 −0.50	>99%, 68%
4	5-Br	freeze-dried cells (1 mg mL^{-1})	0.50	96%, 60%
5	7-Br	freeze-dried cells (3 mg mL^{-1})	0.25	91%, 63%

[a] Conversion of L-bromotryptophan by TnaA was determined by RP-HPLC. [b] Final yield refers to purified product obtained from the two-step cascade.

for biocatalysis.[28] Enzyme assays carried out with 1 mM 6-**5** and ADH/*iso*-propanol for concomitant NADPH regeneration initially gave a purplish suspension at 25 °C. Whilst the substrate was fully consumed, LC-MS indicated 6-bromo-3-hydroxyindole (**6**) as a minor species present (Figure S6A). Not surprisingly, under aerobic conditions, the hydroxylation of 6-**5** directly initiates transformation of the hydroxylated intermediate into the insoluble pigment 6,6′-**2**. Despite low solubility in DMSO and poor ionization abilities, ESI-MS analysis of the colored sediment suggests the presence of 6,6′-dibromoindigo (6,6′-**2**) as the biotransformation product (Figure S6B).

Encouraged by these results, the hydroxylation of **5** was further optimized to obtain an efficient process for the synthesis and isolation of halogenated indigo. Seminal achievements by Fraaije et al. inspired to generate a bifunctional biocatalyst by fusion of mFMO with phosphite dehydrogenase (PTDH).[48–52] N-terminal PTDH genetically fused to mFMO is capable of NADPH regeneration by oxidation of phosphite while the monooxygenase catalyzes the hydroxylation. In case of substrate 6-**5**, the self-sufficient enzyme reached a total conversion of approx. 96% (HPLC), whereas other regeneration systems were less productive (Table S1). Comparing the substrate conversion under optimized conditions revealed that unsubstituted indole causes a 2.5-fold higher TTN than its brominated derivatives (Scheme S1). However, both 5- and 6-bromoindole (5-/6-**5**) are being reasonably converted by PTDH-mFMO with a slight preference for the C6-isomer. Only 7-**5** could not be converted into 7,7′-dibromoindigo.

The optimized biotransformation steps were combined to provide a one-pot cascade allowing stepwise transformation of **3** into dibromoindigo (**2**). In a sequential fashion, halogenation of 3 was followed by elimination and final hydroxylation simply by adding the enzymes and cofactors required for each step without isolation of reaction intermediates (Figure 2 A). Finally, the hydroxylation step reached full conversion after 96 h on 0.1 mmol scale (Figure 2 B). Initial C6-halogenation using the halogenase Thal thus furnishes a purplish-colored solid

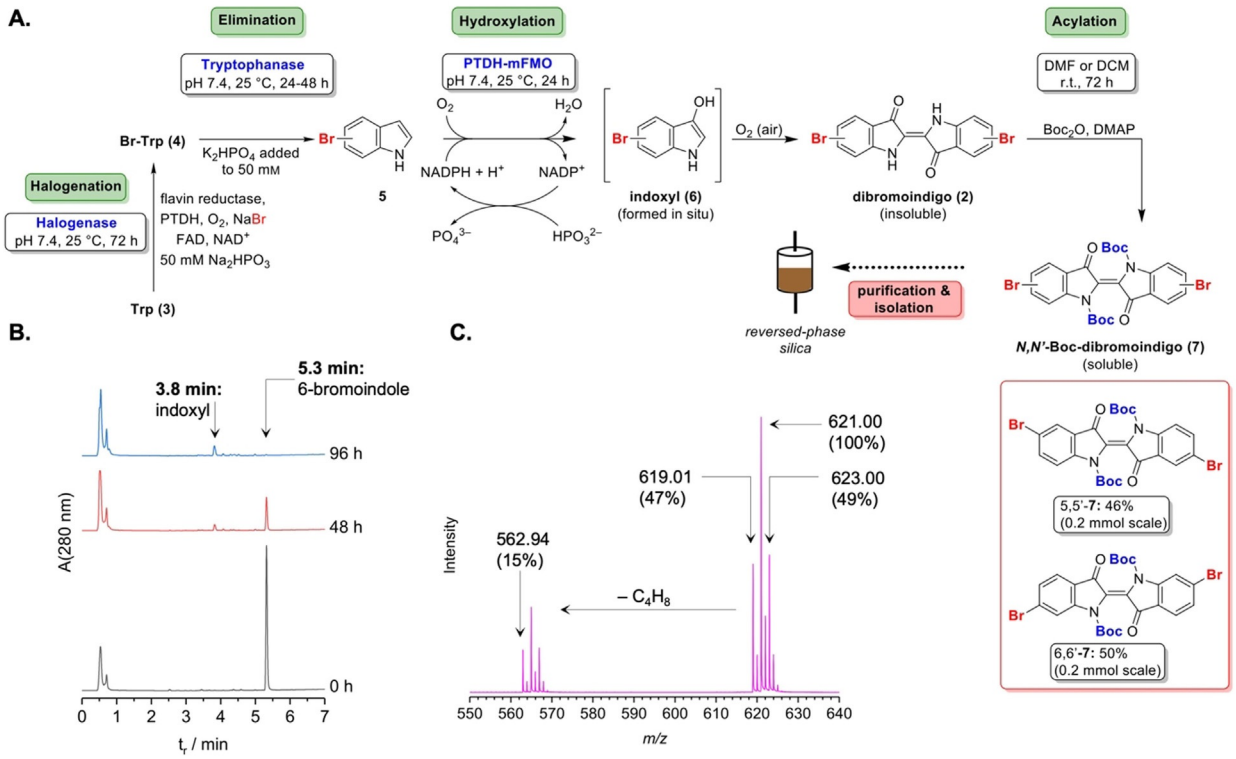

Figure 2. A. Cascade synthesis of Boc-protected dibromoindigo using multiple biocatalysis and Boc protection. The latter step facilitates solubilization and final purification of the protected indigoid. Yields mentioned for **7** refer to the total 4-step cascade; calculations were based on the quantity of substrate **3**. B. HPLC diagram of PTDH-mFMO-catalyzed hydroxylation of 6-**5**. The substrate is continuously converted into insoluble pigment. The intermediary brominated indoxyl is only present in minor quantities while other side products are negligible. C. Identification of *N*,*N*′-Di-Boc-6,6′-dibromoindigo (6,6′-**7**) as the major product of the final acylation step. ESI-ToF MS analysis confirms the identity of the dibrominated compound from the isotope pattern.

pointing to the successful formation of 6,6′-**2** (Figure S8). Likewise, the halogenase PyrH (C5 halogenation) results in 5,5′-**2** as a blue-colored pigment.

As a consequence of its insolubility in aqueous medium, pigment **2** precipitates quantitatively and can be simply harvested by centrifugation. However, its isolation and purification from the biotransformation extract, e.g., from protein precipitate, proves challenging due to its low solubility. In light of a previous study by Sariciftci et al., acylation of the indigo nitrogen enhances solubility by suppression of the intramolecular hydrogen bonds.[53] Hence, subsequent to biocatalysis the crude solid was subjected to *N*,*N*′-Boc protection. As a test system to obtain a suitable procedure applicable to cascade conditions, a crude extract containing **1** was first employed (cf. Supp. Inform. for further details, Table S2). According to these optimized conditions, Boc_2O (15 equiv) and DMAP (3 equiv) were added to a freeze-dried crude extract containing 6,6′-**2** re-suspended in DMF, which led to formation of Boc-protected dibromoindigo (**7**) after stirring for 3 d at r.t. as proven by LC-MS (Figure 2C). The soluble 6,6′-**7** was purified by reversed-phase silica resulting in good purity and an overall yield of 24% after four synthetic steps referring to starting compound **3** (Figure 2A; S9). The final Boc protection step could be optimized by portion-wise addition of Boc_2O/DMAP and the use of CH_2Cl_2 as an alternative solvent. In total, the four-step cascade starting from 0.25 mmol of **3** resulted in an increased yield of 50% on average, based on three independent replicates. Furthermore, a biotransformation on 0.50 mmol scale gave a comparable yield (52%). Likewise, the cascade afforded 5,5′-**7** in a similar yield of 46%. Taking into account that the final product **7** is finally isolated after four sequential reactions, these results indicate a straightforward method towards haloindigos.

We further embarked on investigations to diversify **2** by Pd-catalyzed cross-couplings. Aryl substitution of indigoids is a hitherto unexplored research area. Initially cross-coupling of Boc-protected 6,6′-**7** to the electron-rich 3-aminophenylboronic acid was attempted in order to enhance the polarity of the target compound and to facilitate detection by ESI-MS used as a simple reaction screening. However, as the brominated starting material was prone to Boc cleavage as well as decomposition in basic medium hindering formation of the desired aryl species, we concentrated on arylation of **2** instead.

Even though the cross-coupling of the insoluble unprotected dibromoindigo (**2**) in the crude extract proved more challenging, this approach would provide convenient diversification of the natural dye and potentially enhance solubility. 6-**5** (1.0 μmol) was subjected to hydroxylation and the resulting crude precipitate containing 6,6′-**2** was incubated with 3-aminophenylboronic acid, Pd(sSPhos) and K_3PO_4 at 130 °C in a DMF suspension.

Unexpectedly, LC-MS analysis indicated formation of a mono-methylated diarylindigo whereas dimethylation was not

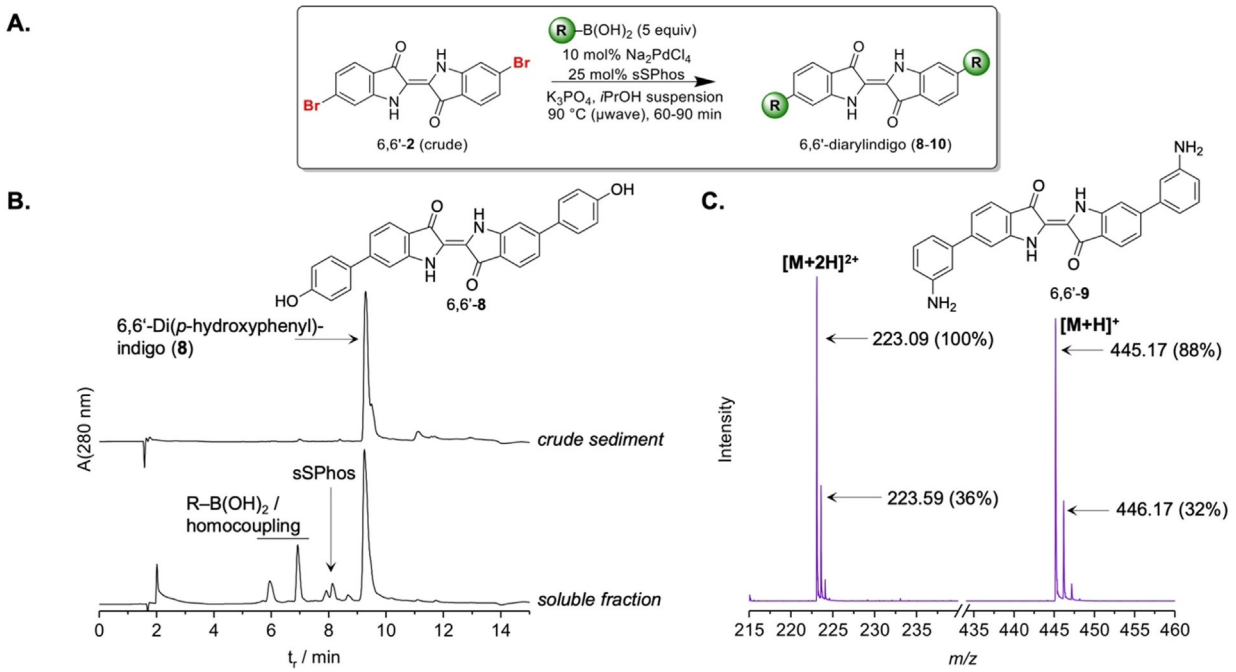

Figure 3. A. Analytical-scale Suzuki–Miyaura cross-coupling of crude 6,6′-dibromoindigo (6,6′-**2**) affording diarylindigo derivatives. B. HPLC (280 nm) of the cross-coupling reaction identifies diarylindigo 6,6′-**8** in the soluble fraction and in the precipitate (re-dissolved in DMF prior to analysis). **C.** ESI-MS data of the reaction of **2** and 3-aminophenylboronic acid prove the successful synthesis of aniline derivative **9** evident from $[M+2H]^{2+}$ ($m/z = 223.09$ calc.) and $[M+H]^{+}$ ($m/z = 445.17$ calc.).

observed (Figure S10). Pd-catalyzed aniline *N*-methylation has been previously described.[54] Cross-coupling at lower temperature (90 °C) in *i*PrOH under microwave irradiation in the presence of 5 equiv of arylboronic acid, 0.1 equiv Na_2PdCl_4, 0.25 equiv sSPhos, and 6 equiv K_3PO_4 gave the unmethylated target compound, accompanied only by minor side products (Figure 3 A/B). Formation of the diarylindigo 6,6′-**8** succeeded when using 4-hydroxyphenylboronic acid: The target diarylindigo among other cross-coupling components and homocoupled product were detectable in the reaction solution as well as in the precipitate (Figure 3 B). Furthermore, MS analysis of the coupling reaction of 3-aminophenylboronic acid perfectly correlates with the twofold coupled aniline derivative 6,6′-**9** whilst not resulting in the methylated side product (Figures 3 C, S11, S12).

To implement indigoid arylation within the cascade, 6,6′-dibromoindigo (6,6′-**2**) was synthesized starting from **3**. The crude extract was subjected to arylation under reflux and Ar atmosphere for 4 h to form diarylindigo. In addition to 6,6′-**8** and 6,6′-**9**, the phenylacetic acid-substituted derivative 6,6′-**10** was obtained by using the corresponding boronic acid (Scheme 3). Its carboxylate salt is also soluble in aqueous basic medium leading to a notable improvement for handling and application of indigoids.

Based on this procedure a small set of 6,6′-diarylindigos was isolated on a low milligram scale upon purification by column chromatography. Product identities were unambiguously confirmed by high-resolution mass spectrometry (cf. Supporting Information, Analytical Data). The HPLC data, instantly recorded after isolation, corroborate sufficient product purity (cf. Supporting Information, Analytical Data). Notably, distinctly separated elution peaks occurred in RP-HPLC for all the diarylindigos under dilute acidic conditions giving different UV/Vis-spectra, but identical mass spectra. This observation indicates the

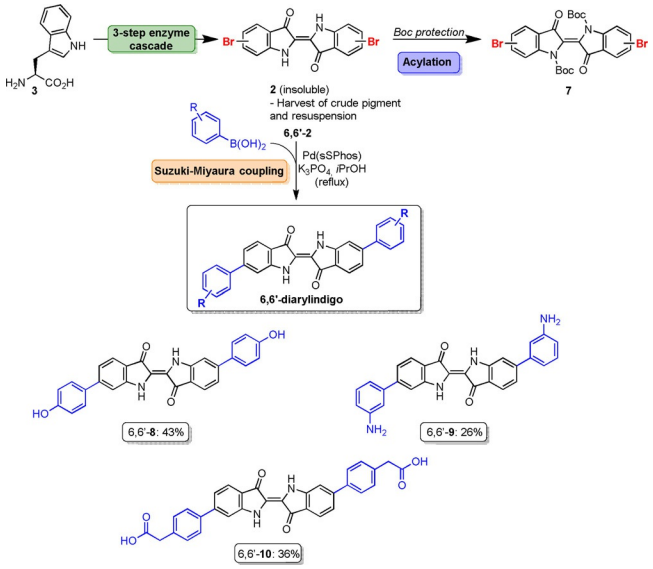

Scheme 3. Overall chemoenzymatic cascade for the synthesis of indigo derivatives. The initial substrate L-tryptophan (**3**) is successively converted into insoluble dibromoindigo (**2**) that is subsequently either *N*-acylated or employed for cross-coupling using a suspension of the crude extract. Particularly, coupling of more polar residues improves compound solubility. Results of 5,5′- and 6,6′-disubstituted indigoids **8**–**10** as well as final product yields referring to the starting material **3** are mentioned.

presence of *cis/trans* isomers (Figures S13–S15).[9] In general, *N*-unsubstituted indigos do not photoisomerize because of dominating and fast deactivation mechanisms.[55] On the other hand, under acidic conditions and in the gas phase a *trans/cis*-protoisomerization has been detected for indigo and its bisimine derivatives.[55] The presence of the *trans/cis*-isomers in the diarylindigoids suggests that aryl substitutions at the indigo core reduce the double bond character of the central C=C bond, thus facilitating isomerization in the protonated state (Scheme S2).[55] NMR characterization of the aryl products proved challenging, probably as a consequence of the resultant low quantities along with isomerism and a potential light sensitivity. For example, ^{1}H- and ^{13}C-NMR signals could be clearly assigned for 6,6′-**8** and 6,6′-**10**. Additional peaks detected in the spectra originate from isomerization as well as minor impurities that were taken into account when calculating the yields (Table 1, Scheme 3). Cross-couplings using 5,5′-**2** were less efficient and potential products could not be isolated in satisfactory purities.

UV/Vis and fluorescence spectra were recorded to study the spectroscopic properties of the novel diarylindigo derivatives. Substituents at the benzene ring of the indigo moiety do not have a pronounced effect on the UV/Vis absorption. +M Substituents like halogens or methoxy groups at the 5,5′- or 7,7′-positions of indigo are supposed to cause a bathochromic shift, while at the 6,6′-positions a hypsochromic shift is expected. This characteristic is mainly known for Tyrian purple (6,6′-**2**), which has its visible band at lower wavelengths than indigo (**1**).[56] In case of diarylindigoids, the aromatic rings mainly stabilize the coplanar conformation of the molecule with a marginal mesomeric effect; however a fine-tuning of the maximal wavelength might be possible by changing the peripheral substituents.[57]

In DMSO, only diarylindigo 6,6′-**10** with the *para*-carboxymethylbenzoic acid moiety shows an intense band in the deep red region at 626 nm similar to the band of **1** at 619 nm (Figure 4A, dashed line). Besides, a second intense band at 384 nm is different to the shoulder observed for indigo (**1**) at 333 nm. Another band appeared at 318 nm, while **1** shows a signal below 300 nm. Notably 6,6′-**10** is soluble in water, in which a strong hypsochromic effect was observed. The change of solvent from DMSO to water did not change the absorption maximum at 624 nm.

For the other arylindigo derivatives, a hypsochromic effect in comparison to indigo (**1**) was obvious. Trace amounts of water might be the reason, as **8** and **9** turned out to be rather hygroscopic. The aminophenyl-substituted indigoid (6,6′-**9**) shows strong hypsochromic and bathochromic shifts to 597 nm and 650 nm, respectively (Figure S16). On the contrary, the hydroxyaryl derivative (6,6′-**8**) shows a different tendency with a maximum at 630 nm for 6,6′-**8**.

Generally, indigo and its derivatives often suffer from low fluorescence and low quantum yields due to a dominant radiationless decay (e.g. Figure S17).[55] Interestingly, 6,6′-**10** shows intense fluorescence emission at 664 nm that is even three times higher than that of indigo (**1**) under identical experimental conditions (Figure 4A, full line, Figure 4C). However, in water this fluorescence band does not occur, so that 6,6′-**10** merely shows a significant emission at 425 nm pointing to an influence of the solvent on the fluorescence properties of this compound (Figure 4B, full line). A qualitative comparison of the fluorescence intensity of the other 6,6′-derivatives in DMSO

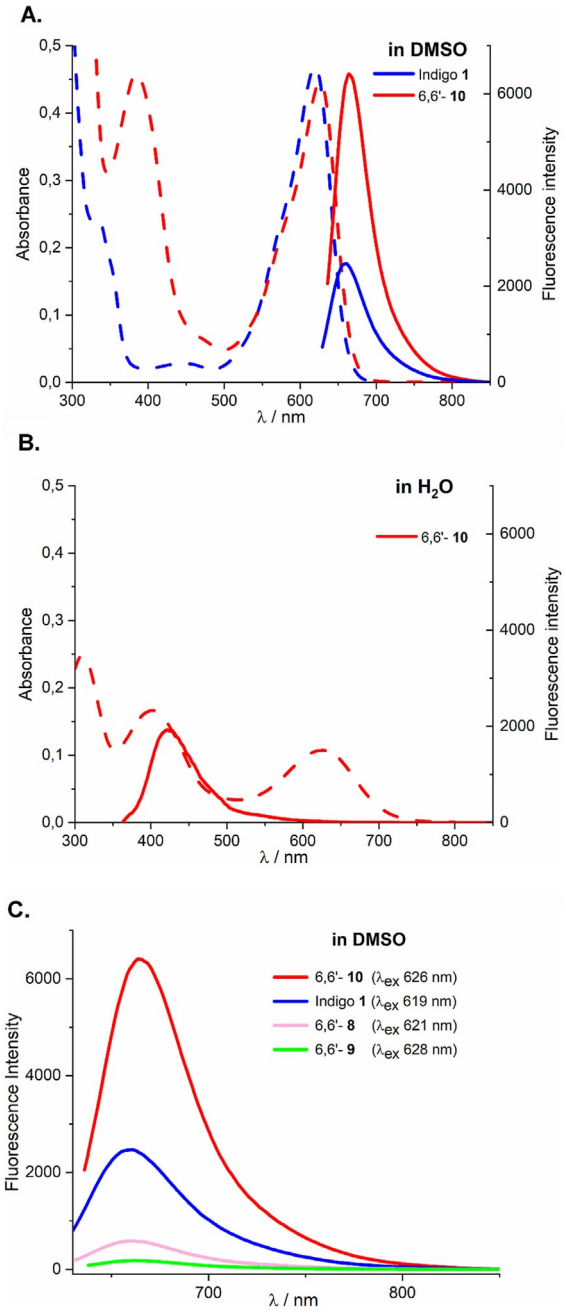

Figure 4. Solvent-dependent UV/Vis absorbance (– – –) and fluorescence emission (——) spectra of 6,6′-**10** and indigo (**1**). A. in DMSO. B. in water; only 6,6′-**10** is soluble (λ_{ex} = 320 nm). C. A qualitative comparison of the fluorescence intensity of the 6,6′-derivatives at around 660 nm in DMSO is shown (25 μM, 20 °C), spectra were acquired at optimum excitation wavelengths of each compound. Further spectra and experimental details are presented in the Supporting Information (S16, S17). Identical experimental conditions were applied for all compounds analyzed (25 μM, 20 °C; cf. Supporting Information).

under comparable acquisition conditions showed that their fluorescence intensity at around 660 nm is marginal (Figure 4C).[58] The initial evaluation of the spectroscopic characteristics of the arylindigoids synthesized in this work reveals the complexity of their behavior indicating different patterns than those known for the reference compound **1**. A profound evaluation of the observed photophysical properties, as well as their photoisomerization properties is in progress.

In conclusion, sequential biocatalytic C–H activation implemented in a one-pot cascade enables stepwise transformation of tryptophan (**3**) into a versatile array of indigoids. Besides that, a facile synthesis of haloindoles was established that is suitable for a range of synthetic purposes. The modular cascade of multiple biocatalytic steps and acylation described here renders 5,5′- and 6,6′-dibromoindigo as easy-to-handle Boc-protected derivatives in good overall yields after four steps. Suzuki–Miyaura coupling enabling diversification as the final reaction step was exemplified for a small set of 6,6′-diarylindigos. In particular, cross-coupling using aryl halide **2** can be directly performed in the crude extract resulting from the previous biotransformation. This chemoenzymatic route offers an alternative approach to previously reported approaches which make use of early-stage cross coupling instead.[57] Moreover, characterization of the novel indigoids unveils interesting photophysical features. The methodology presented herein underscores the potential of enzymatic halogenation and oxyfunctionalization for site-selective aryl diversification. The cascade offers an attractive means to manipulate indigoid properties towards applications in material science. In future, these tools will be expanded further using enzyme and reaction engineering to provide sustainable access towards tailor-made, nature-derived materials.

Acknowledgements

The authors are grateful to Anke Nieß, Anika Kleine and Marco Wißbrock for experimental assistance. Heiko Ihmels (Siegen) is acknowledged for helpful discussions. Open access funding enabled and organized by Projekt DEAL.

Conflict of interest

The authors declare no conflict of interest.

Keywords: cascade · C–H functionalization · halogenase · heterocycles · monooxygenase

[1] M. Bandini, A. Eichholzer, *Angew. Chem. Int. Ed.* **2009**, *48*, 9608 – 9644; *Angew. Chem.* **2009**, *121*, 9786 – 9824.
[2] M. Klessinger, W. Lüttke, *Tetrahedron* **1963**, *19*, 315 – 335.
[3] L. Serrano-Andrés, B. O. Roos, *Chem. Eur. J.* **1997**, *3*, 717 – 725.
[4] E. D. Głowacki, G. Voss, L. Leonat, M. Irimia-Vladu, S. Bauer, N. S. Sariciftci, *Isr. J. Chem.* **2012**, *52*, 540 – 551.
[5] M. Irimia-Vladu, E. D. Głowacki, P. A. Troshin, G. Schwabegger, L. Leonat, D. K. Susarova, O. Krystal, M. Ullah, Y. Kanbur, M. A. Bodea, V. F. Razumov, H. Sitter, S. Bauer, N. S. Sariciftci, *Adv. Mater.* **2012**, *24*, 375 – 380.
[6] E. D. Głowacki, D. H. Apaydin, Z. Bozkurt, U. Monkowius, K. Demirak, E. Tordin, M. Himmelsbach, C. Schwarzinger, M. Burian, R. T. Lechner, N. Demitri, G. Voss, N. S. Sariciftci, *J. Mater. Chem. C* **2014**, *2*, 8089 – 8097.
[7] C.-Y. Huang, A. Bonasera, L. Hristov, Y. Garmshausen, B. M. Schmidt, D. Jacquemin, S. Hecht, *J. Am. Chem. Soc.* **2017**, *139*, 15205 – 15211.
[8] C. Petermayer, S. Thumser, F. Kink, P. Mayer, H. Dube, *J. Am. Chem. Soc.* **2017**, *139*, 15060 – 15067.
[9] L. A. Huber, P. Mayer, H. Dube, *ChemPhotoChem* **2018**, *2*, 458 – 464.
[10] J. L. Wolk, A. A. Frimer, *Molecules* **2010**, *15*, 5473 – 5508.
[11] M. Hönig, P. Sondermann, N. J. Turner, E. M. Carreira, *Angew. Chem. Int. Ed.* **2017**, *56*, 8942 – 8973; *Angew. Chem.* **2017**, *129*, 9068 – 9100.
[12] F. Rudroff, M. D. Mihovilovic, H. Gröger, R. Snajdrova, H. Iding, U. T. Bornscheuer, *Nat. Catal.* **2018**, *1*, 12 – 22.
[13] S. P. France, L. J. Hepworth, N. J. Turner, S. L. Flitsch, *ACS Catal.* **2017**, *7*, 710 – 724.
[14] U. T. Bornscheuer, G. W. Huisman, R. J. Kazlauskas, S. Lutz, J. C. Moore, K. Robins, *Nature* **2012**, *485*, 185 – 194.
[15] J. Dong, E. Fernández-Fueyo, F. Hollmann, C. E. Paul, M. Pesic, S. Schmidt, Y. Wang, S. Younes, W. Zhang, *Angew. Chem. Int. Ed.* **2018**, *57*, 9238 – 9261; *Angew. Chem.* **2018**, *130*, 9380 – 9404.
[16] M. T. Reetz, *J. Am. Chem. Soc.* **2013**, *135*, 12480 – 12496.
[17] R. Fasan, *ACS Catal.* **2012**, *2*, 647 – 666.
[18] Y. Wei, E. L. Ang, H. Zhao, *Curr. Opin. Chem. Biol.* **2018**, *43*, 1 – 7.
[19] S. Chakrabarty, Y. Wang, J. C. Perkins, A. R. H. Narayan, *Chem. Soc. Rev.* **2020**, *49*, 8137 – 8155.
[20] B. D. Ensley, B. J. Ratzkin, T. D. Osslund, M. J. Simon, L. P. Wackett, D. T. Gibson, *Science* **1983**, *222*, 167 – 169.
[21] J. Y. Kim, K. Lee, Y. Kim, C.-K. Kim, K. Lee, *Lett. Appl. Microbiol.* **2003**, *36*, 343 – 348.
[22] Q.-S. Li, U. Schwaneberg, P. Fischer, R. D. Schmid, *Chem. Eur. J.* **2000**, *6*, 1531 – 1536.
[23] A. Meyer, M. Würsten, A. Schmid, H.-P. E. Kohler, B. Witholt, *J. Biol. Chem.* **2002**, *277*, 34161 – 34167.
[24] Z. Pengpai, H. Sheng, M. Lehe, L. Yinlin, J. Zhihua, H. Guixiang, *Appl. Biochem. Biotechnol.* **2013**, *171*, 93 – 103.
[25] A. Çelik, R. E. Speight, N. J. Turner, *Chem. Commun.* **2005**, 3652 – 3654.
[26] P. P. Kelly, A. Eichler, S. Herter, D. C. Kranz, N. J. Turner, S. L. Flitsch, *Beilstein J. Org. Chem.* **2015**, *11*, 1713 – 1720.
[27] D. A. Vargas, A. Tinoco, V. Tyagi, R. Fasan, *Angew. Chem. Int. Ed.* **2018**, *57*, 9911 – 9915; *Angew. Chem.* **2018**, *130*, 10059 – 10063.
[28] H. S. Choi, J. K. Kim, E. H. Cho, Y. C. Kim, J. I. Kim, S. W. Kim, *Biochem. Biophys. Res. Commun.* **2003**, *306*, 930 – 936.
[29] G. H. Han, G. H. Gim, W. Kim, S. I. Seo, S. W. Kim, *J. Biotechnol.* **2013**, *164*, 179 – 187.
[30] T. Heine, C. Großmann, S. Hofmann, D. Tischler, *Biol. Chem.* **2019**, *400*, 939 – 950.
[31] S. Fräbel, B. Wagner, M. Krischke, V. Schmidts, C. M. Thiele, A. Staniek, H. Warzecha, *Metab. Eng.* **2018**, *46*, 20 – 27.
[32] S. Namgung, H. A. Park, J. Kim, P.-G. Lee, B.-G. Kim, Y.-H. Yang, K.-Y. Choi, *Dyes Pigm.* **2019**, *162*, 80 – 88.
[33] V. Weichold, D. Milbredt, K.-H. van Pée, *Angew. Chem. Int. Ed.* **2016**, *55*, 6374 – 6389; *Angew. Chem.* **2016**, *128*, 6482 – 6498.
[34] H. Minges, N. Sewald, *ChemCatChem* **2020**, *12*, 4450 – 4470.
[35] J. T. Payne, M. C. Andorfer, J. C. Lewis, *Angew. Chem. Int. Ed.* **2013**, *52*, 5271 – 5274; *Angew. Chem.* **2013**, *125*, 5379 – 5382.
[36] J. T. Payne, C. B. Poor, J. C. Lewis, *Angew. Chem. Int. Ed.* **2015**, *54*, 4226 – 4230; *Angew. Chem.* **2015**, *127*, 4300 – 4304.
[37] A.-C. Moritzer, H. Minges, T. Prior, M. Frese, N. Sewald, H. H. Niemann, *J. Biol. Chem.* **2019**, *294*, 2529 – 2542.
[38] M. Frese, N. Sewald, *Angew. Chem. Int. Ed.* **2015**, *54*, 298 – 301; *Angew. Chem.* **2015**, *127*, 302 – 305.
[39] C. Schnepel, H. Minges, M. Frese, N. Sewald, *Angew. Chem. Int. Ed.* **2016**, *55*, 14159 – 14163; *Angew. Chem.* **2016**, *128*, 14365 – 14369.
[40] J. Latham, J.-M. Henry, H. H. Sharif, B. R. K. Menon, S. A. Shepherd, M. F. Greaney, J. Micklefield, *Nat. Commun.* **2016**, *7*, 11873.
[41] A. D. Roy, S. Grüschow, N. Cairns, R. J. M. Goss, *J. Am. Chem. Soc.* **2010**, *132*, 12243 – 12245.
[42] S. V. Sharma, X. Tong, C. Pubill-Ulldemolins, C. Cartmell, E. J. A. Bogosyan, E. J. Rackham, E. Marelli, R. B. Hamed, R. J. M. Goss, *Nat. Commun.* **2017**, *8*, 229.
[43] C. Schnepel, I. Kemker, N. Sewald, *ACS Catal.* **2019**, *9*, 1149 – 1158.

[44] P. R. Neubauer, C. Widmann, D. Wibberg, L. Schröder, M. Frese, T. Kottke, J. Kalinowski, H. H. Niemann, N. Sewald, *PLoS ONE* **2018**, *13*, e0196797.
[45] W. A. Newton, Y. Morino, E. E. Snell, *J. Biol. Chem.* **1965**, *240*, 1211 – 1218.
[46] G. Li, K. D. Young, *Microbiology* **2013**, *159*, 402 – 410.
[47] C. H. Suelter, E. E. Snell, *J. Biol. Chem.* **1977**, *252*, 1852 – 1857.
[48] A. Rioz-Martínez, M. Kopacz, G. de Gonzalo, D. E. Torres Pazmiño, V. Gotor, M. W. Fraaije, *Org. Biomol. Chem.* **2011**, *9*, 1337 – 1341.
[49] T. W. Johannes, R. D. Woodyer, H. Zhao, *Biotechnol. Bioeng.* **2007**, *96*, 18 – 26.
[50] Y. Zou, H. Zhang, J. S. Brunzelle, T. W. Johannes, R. Woodyer, J. E. Hung, N. Nair, W. A. van der Donk, H. Zhao, S. K. Nair, *Biochemistry* **2012**, *51*, 4263 – 4270.
[51] D. E. Torres Pazmiño, R. Snajdrova, B.-J. Baas, M. Ghobrial, M. D. Mihovilovic, M. W. Fraaije, *Angew. Chem. Int. Ed.* **2008**, *47*, 2275 – 2278; *Angew. Chem.* **2008**, *120*, 2307 – 2310.
[52] D. E. Torres Pazmiño, A. Riebel, J. de Lange, F. Rudroff, M. D. Mihovilovic, M. W. Fraaije, *ChemBioChem* **2009**, *10*, 2595 – 2598.
[53] E. D. Głowacki, G. Voss, K. Demirak, M. Havlicek, N. Sünger, A. C. Okur, U. Monkowius, J. Gąsiorowski, L. Leonat, N. S. Sariciftci, *Chem. Commun.* **2013**, *49*, 6063 – 6065.
[54] L. Jiang, F. Guo, Y. Wang, J. Jiang, Y. Duan, Z. Hou, *Asian J. Org. Chem.* **2019**, *8*, 2046 – 2049.
[55] J. Seixas de Melo, A. P. Moura, M. J. Melo, *J. Phys. Chem. A* **2004**, *108*, 6975 – 6981.
[56] J. Formanek, *Angew. Chem.* **1928**, *41*, 1133 – 1141.
[57] J. H. Porada, J.-M. Neudörfl, D. Blunk, *New J. Chem.* **2015**, *39*, 8291 – 8301.
[58] D. Farka, M. Scharber, E. D. Głowacki, N. S. Sariciftci, *J. Phys. Chem. A* **2015**, *119*, 3563 – 3568.

Manuscript received: December 3, 2020
Accepted manuscript online: January 26, 2021
Version of record online: February 26, 2021